Magnetic anisotropy of epitaxial Co_2Fe-Ge Heusler alloy films on MgO (100) substrates

A. N. Pogorily,[1,a] A. F. Kravets,[1,2,b] V. V. Nevdacha,[1] D. Y. Podyalovskiy,[1] S. M. Ryabchenko,[3] V. M. Kalita,[3] M. M. Kulik,[3] A. F. Lozenko,[3] A. Ya. Vovk,[4] M. Godinho,[4] L. Maurel,[5] J. A. Pardo,[5] C. Magen,[5] and V. Korenivski[2]
[1]*Institute of Magnetism, National Academy of Sciences of Ukraine, 03680 Kyiv, Ukraine*
[2]*Nanostructure Physics, Royal Institute of Technology, 10691 Stockholm, Sweden*
[3]*Institute of Physics, National Academy of Sciences of Ukraine, 03680 Kyiv, Ukraine*
[4]*BioISI Biosystems and Integrative Sciences Institute, Faculdade de Cincias, Universidade de Lisboa, Campo Grande, 1749-016 Lisboa, Portugal*
[5]*Instituto de Nanociencia de Aragn, Universidad de Zaragoza, 50018 Zaragoza, Spain*

(Presented 1 November 2016; received 23 September 2016; accepted 1 December 2016; published online 3 March 2017)

Films of Co_2Fe-Ge Heusler alloy with variable Ge concentration deposited on monocrystalline MgO (100) substrates by magnetron co-sputtering are investigated using microstructural, morphological, magnetometric, and magnetic resonance methods. The films were found to grow epitaxially, with island-like or continuous-layer morphology depending the Ge-content. The ferromagnetic resonance data versus out-of-plane and in-plane angle indicate the presence of easy plane and 4-fold in-plane anisotropy. The magnetometry data indicate additional weak 2-fold in-plane anisotropy and pronounced at low fields rotatable anisotropy. The observed magnetic anisotropy properties discussed in correlation with the microstructure and morphology of the films. [http://dx.doi.org/10.1063/1.4978209]

Some of the full-Heusler alloys (FHA) are half-metallic ferromagnets,[1] described by the formula X_2YZ, where X and Y are transition metals and Z is an sp group element. The conductivity bands electrons in half-metallic ferromagnets are 100% spin polarized.[2] Therefore, FHA materials are promising for use as electrodes in magnetic tunnel junctions and spin valves.[3–5] Use of FHA in spintronic devices requires knowledge and control of their magnetic properties and, in particular, their magnetic anisotropy. Our previous work[6] focused on preparation, structural and magnetic characterization of nanocrystalline FHA $(Co_2Fe)_xGe_{100-x}$ (x is mole fraction) (CFG) on oxidized Si substrates. Here we report the results on $(Co_2Fe)_xGe_{100-x}$ epitaxially grown on MgO (100) substrates.

$(Co_2Fe)_xGe_{100-x}$ films were grown on monocrystalline MgO (001) substrates, in the same deposition run as the $(Co_2Fe)_xGe_{100-x}$ films on oxidized (001) Si.[6] The growth of $(Co_2Fe)_xGe_{100-x}$ of nominal thickness d = 50 nm was done at 500°C using DC magnetron co-sputtering from separate targets of Co_2Fe and Ge. The base pressure was $\sim 5 \times 10^{-8}$ Torr and the Ar pressure used during deposition was 5 mTorr. The film compositions were adjusted by varying the Co_2Fe and Ge deposition rates, with relevant calibration by thickness profilometry and EDX analysis. To prevent nonuniform grows of the films the sample holder was rotated at 32 rpm during the film deposition and cooling down to ambient temperature. The actual composition of the films was determined using x-ray fluorescence (XRF) and is listed in Table I. The crystal structure of the films was analyzed using x-ray diffraction (XRD) in the $\theta/2\theta$ geometry with CuKα radiation of wavelength

[a]Electronic mail: apogorily@aol.com
[b]Electronic mail: anatolii@kth.se

TABLE I. Structure and magnetic properties of $(Co_2Fe)_xGe_{100-x}$ films on (100) MgO substrate: x is the mole fraction, a is the lattice parameter, Δ is the FMR linewidth, d is the thickness, r is the roughness, ρ is the density, H_C is the coercive force, M is the magnetization.

Sample	x (m.f.%)	a (Å)	Δ (deg.)	d (nm)	r (nm)	ρ (g/cm^3)	H_C (Oe)	M (emu/cm^3)
A	53.4±0.1	5.738	0.360	53.31	2.451	6.00114	180	640±0.5%
B	56.9±0.5	5.734	0.448	54.44	2.999	6.00016	166	700±0.5%
C	56.9±0.5	5.730	0.427	38.42	1.209	7.66778	75	1100±0.5%
D	70.6±0.3	5.712	0.513	41.35	0.779	8.49235	25	1270±0.5%
E	73.0±0.4	5.707	0.558	43.50	1.411	8.66029	20	1260±0.5%
F	76.3±0.3	5.706	0.492	40.86	0.148	8.56940	22	1240±0.5%

1.5406Å. The films were grown on substrates of 10×10 mm^2, which were later cut to approximately 3×5 mm^2 for characterization and measurements. The crystallographic axes of the substrates had somewhat different orientation with respect to the side boundaries of the samples during measurements. Cross-sectional high-resolution (HRTEM) and scanning (STEM) transmission electron microscopy were performed on FEI Tecnai F30. The magnetization measurements were performed using SQUID and VSM magnetometers, at room temperature. The measured magnetization component was along the applied field, M_H, or the one along the pickup-coils axis (for the case of zero applied field). Ferromagnetic resonance (FMR) measurements were done with a Bruker EMX system at 9.87 GHz.

The thickness of the films was estimated using X-ray reflectivity (XRR). The XRR data were analyzed using the Leptos Bruker software to obtain the thickness, surface roughness, and density of the films. These are listed in Table I. The periodicity near $2\theta \approx 1.5$–2.5° vanished for some of the films, which can be due to formation of a thin oxide layer at the surface, clearly seen in samples D and F, in particular. The density of the surface-oxide layer was used as a free parameter in the cases where the critical angle did not yield a good approximation. Since CFG is not a stoichiometric alloy, Co_3O_4 was chosen as the base oxide composition. The results of the data analysis have shown that, although the films were deposited under the same conditions, the resulting film density may differ for different substrates and therefore the thickness can be different too.

Symmetrical $\theta/2\theta$ scans show only 002 and 004 reflections. Peaks from secondary phases or different plane families were not detected. This proves that the film is composed only of CFG with epitaxial relationship: (001)CFG ||(001)MgO. In-plane orientation was determined through the ϕ-scan of the asymmetrical 022 reflection from CFG. Four peaks were observed at $\pm 45^\circ$ and $\pm 135^\circ$ (taking the MgO [100] in-plane direction for the origin of ϕ), which confirms the in-plane epitaxial relationship: [110]CFG||[100]MgO. This 45° in-plane rotation of the CFG cubic cell relative to the MgO cubic cell was expected, since the ratio between the CFG and MgO lattice parameters is close to $\sqrt{2}$. Symmetric scans $\theta/2\theta$ about the 004 peak were performed for determining the out-of-plane lattice parameter, listed in Table I, which decreases monotonically with increasing x. The value of this lattice parameter for bulk Co_2FeGe is 5.75Å, which indicates that the samples with lower x (A and B) are closer to stoichiometric Co_2FeGe. Rocking curves were measured for the 004 reflection. The obtained values of Full Width at the Half Maximum (FWHM), Δ, are listed in Table I and show no significant differences among the films within the entire series. Films with lower x (higher lattice parameter and therefore smaller mismatch with the substrate) show generally higher crystal quality.

The most interesting asymmetric reflections are those exclusive from $L2_1$ full-Heusler ordering, such as 111 and 113. The reflection 113 is found only in the fully ordered $L2_1$ phase or disordered DO_3 phase (Co occupies Fe sites). The latter is allowed only if there is a significant Co excess. However, 113 reflection is absent in A2 or B2 disordered phases. The result of the $\theta/2\theta$ scans around 113 reflection in grazing incidence shown in Fig. 1. It is seen that sample A has the highest amount of phase $L2_1$, followed by samples C, B, E, D, and finally F.

The HRTEM analysis of samples A, C, and F show that film A has an island-like morphology; film C forms an island-like but continuous layer; film F is a continuous layer (Fig. 2 a,b,c). For all

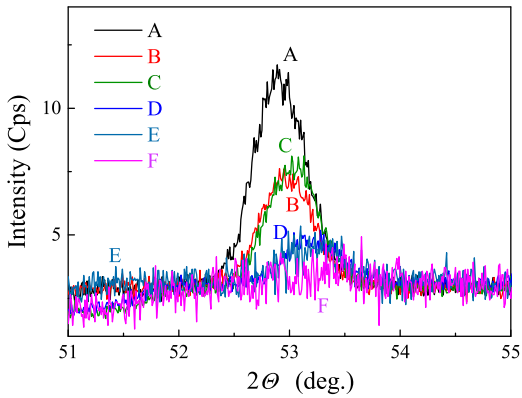

FIG. 1. $\theta/2\theta$ scans around 113 reflection in grazing incidence.

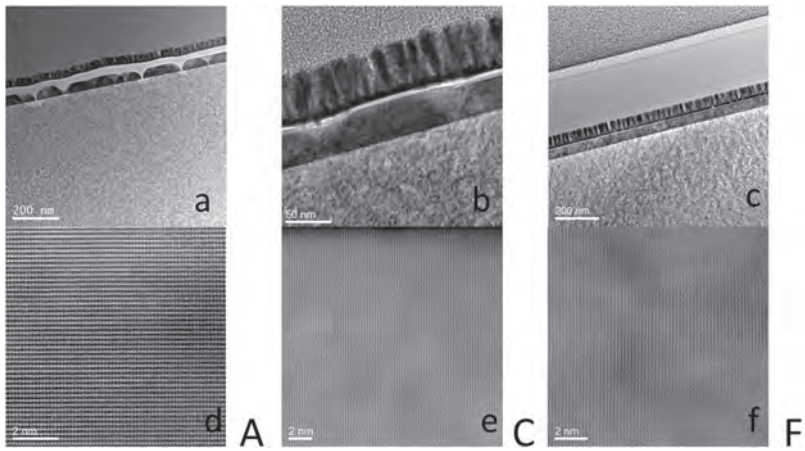

FIG. 2. TEM images of $(Co_2Fe)_xGe_{100-x}$ samples A, C and F.

films, island-like or continuous, the growth is epitaxial in nature, evidenced by the STEM images of the samples (Fig. 2 d,e,f).

The main result of our earlier study of $(Co_2Fe)_xGe_{100-x}$ films deposited onto oxidized (001) Si substrates was the observation of the rotatable magnetic anisotropy. In addition, significantly off-stoichiometric films showed additional 4-fold and 2-fold anisotropy, even though the films were grown on the amorphous surface of a relatively thick (1 μm) oxide layer of SiO_2. This behavior was explained[6] by texturing of the films caused by a mechanism described in Ref. 7, since the growth was done at relatively high temperature and annealing could take place during the growth.

FMR measurements of the CFG/MgO films yield spectra consistent with shape induced easy plane anisotropy ($N_{zz} = 4\pi$, $N_{xx} = N_{yy} = 0$, with the z-axis along the films normal and the x- and y-axes in the film plane). The spectra were recorded at fixed φ_H and various θ_H, where θ_H and φ_H are the angles between the applied field and, respectively, the films normal and the long edge of a rectangular sample. The measured value of $4\pi M_S^{\text{eff}}$, where M_S^{eff} is the effective saturation magnetization determining the easy-plane anisotropy, is greater than 10 kOe for all samples. A series of FMR spectra were measured for different φ_H and fixed $\theta_H = 90°$, i.e. with the external field applied in the film plane. All samples demonstrated a pronounced angular dependence of the resonance field, shown in Fig. 3. The mean resonance field values, averaged over φ_H, for samples A, B, and C are somewhat higher than that for samples D, E, and F. This indicates a somewhat higher $4\pi M_S^{\text{eff}}$ in samples A-C as compared with that in samples D-F, and can be due to the TEM-confirmed island-like film morphology in samples A, C (and likely B). It is clearly seen in Fig. 3 that all samples possess 4-fold

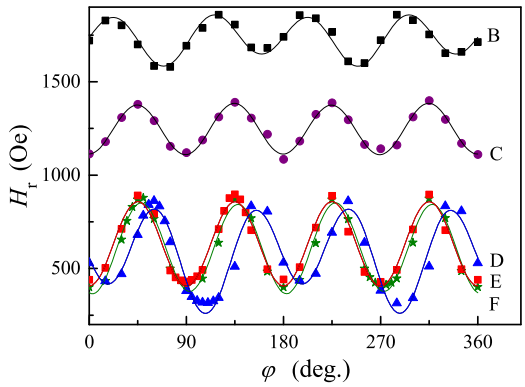

FIG. 3. Angular dependence of in-plane FMR resonance fields.

anisotropy in the plane, with approximately same amplitude of the angular dependence of the resonance field. This behavior suggests that all films have cubic magnetocrystalline anisotropy, with one axis along the films normal and the other two cubic axes at certain angles to the (001) oriented substrate.

The films additionally exhibit 2-fold anisotropy in the plane, which is smaller than the 4-fold anisotropy and is different in magnitude for different films. For example, the 2-fold anisotropy is practically absent (within the measurement accuracy) in samples C, E, and F. No correlation is found between the amplitude of the 180°-component of the angular dependence of the resonance field and the molar fraction of Co_2Fe in the samples. The easy axis of the 2-fold anisotropy term is close or coincides with one of the easy axes of the 4-fold anisotropy. These results qualitatively agree with those reported for a film of other FHAs grown onto (001)-oriented substrates of monocrystalline MgO.[8–15]

Hysteresis curves measured using a VSM at $\theta_H = 0$ are almost linear at low fields ($|H| < 4\pi M_S^{\text{eff}}$), which is in good correspondence with easy-plane anisotropy. Hysteresis curves measured for various angles φ_H in the films plane (with $\theta_H = 90°$) show large remanent magnetization for all in-plane directions, with the shape of the curves close to rectangular. No sample showed a 90°-component in the angular dependence of the coercive field, H_C, regardless of its clear presence in the FMR deduced anisotropy. We observed a weakly defined 180°-component in the H_C-vs-φ data for samples B and C, barely above the experimental uncertainty.

A series of precision measurements were performed using a SQUID magnetometer, and yielded the coercive fields and the magnetization values listed in Table I. The magnetization was calculated from the measured saturation magnetic moments using the film thickness values obtained with XRR. The nearly stoichiometric samples A and B have coercive fields 180 Oe and 166 Oe. The samples significantly deviating from stoichiometry (D, E, and F) have coercive fields 20–25 Oe. SQUID hysteresis curves for samples A and F are shown in Fig. 4 a. The observed significant difference is likely caused by the island-like morphology of the nearly stoichiometric films.

The effect of preceding field-saturation on the remanent moment of the films was studied using the method employed earlier in Ref. 6. A saturating magnetic field was applied in the film plane, then the magnetization component along the field direction and the component perpendicular to the plane of the pickup coils were measured. The applied field was subsequently removed and the magnetization component perpendicular to the plane of the pickup coils was measured while the film was rotated about its normal (varying in-plane angle φ) (Fig. 4 b). These measurements were analyzed to obtain the remanent moment as a function of the saturation direction $M_r(\varphi_{H\text{sat}})$ as well as its orientation $\varphi_0(\varphi_{H\text{sat}})$, with $\varphi_{H\text{sat}}$ being the angle between the in-plane axis x and the saturating field direction. The obtained results indicate that, within the experimental accuracy, $\varphi_0(\varphi_{H\text{sat}}) = \varphi_{H\text{sat}}$, i.e., the direction of the remanent moment coincides with the direction of the saturating field. We conclude that in the region of low fields, in the vicinity of the coercive field, the system exhibits rotatable anisotropy with the easy axis following the direction of the field used immediately prior

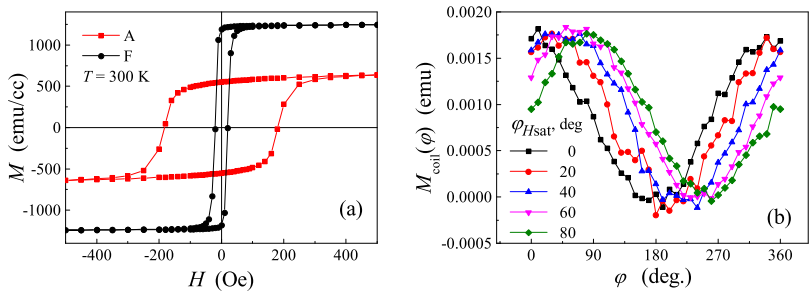

FIG. 4. (a) Magnetic hysteresis loops for samples A and F. (b) Angular dependence of the projection of the remanent magnetic moment of the films on the direction of measurement, after saturating the film magnetization along different in-plane directions, $\varphi_{H\mathrm{sat}}$, for film A.

to saturate the system, similar to the behavior found in the films of CFG on amorphous Si/SiO_2 substrates.[6] This rotatable anisotropy masks the cubic crystallographic anisotropy, which however becomes noticeable at significantly higher fields, of magnitude close to the FMR fields.

In summary, we observe that all investigated films exhibit 4-fold anisotropy, which is magnetocrystalline in nature. Also significantly weaker 2-fold anisotropy was observed in the plane. The easy axis of the 2-fold anisotropy is either close to or coincides with one of the easy axes of the 4-fold anisotropy. The full set of the magnetostatic measurements and, in particular, the magnetization-vs-angle data indicate a presence in the films of additional rotatable anisotropy, with the easy axis that follows the direction of the applied saturating magnetic field preceding the measurement. These anisotropy properties are correlated with the microstructure and morphology of the FHA Co_2Fe-Ge films.

ACKNOWLEDGMENTS

Support from the Swedish Stiftelse Olle Engkvist Byggmästare, the Swedish Research Council (VR grant 2014-4548), the Portugal FCT Ciencia 2008 program (A. Vovk), and the National Academy of Sciences of Ukraine (project 0115U00974) are gratefully acknowledged.

[1] C. Felser, G. H. Fecher, and B. Balke, Angew. Chem. Int. Ed. **46**, 668 (2007).
[2] R. A. de Groot, F. M. Mueller, P. G. v. Engen, and K. H. J. Buschow, Phys. Rev. Lett. **50**, 2024 (1983).
[3] T. Marukame, T. Ishikawa, S. Hakamata, K. Matsuda, T. Uemura, and M. Yamamoto, Appl. Phys. Lett. **90**, 012508 (2007).
[4] N. Tezuka, N. Ikeda, S. Sugimoto, and K. Inomata, Appl. Phys. Lett. **89**, 252508 (2006).
[5] T. M. Nakatani, T. Furubayashi, S. Kasai, H. Sukegawa, Y. K. Takahashi, S. Mitani, and K. Hono, Applied Physics Letters **96**, 212501 (2010).
[6] S. M. Ryabchenko, V. M. Kalita, M. M. Kulik, A. F. Lozenko, V. V. Nevdacha, A. N. Pogorily, A. F. Kravets, D. Y. Podyalovskiy, V. A. Ya., R. P. Borges, M. Godinho, and V. Korenivski, J. Phys.: Cond. Matt. **25**, 416003 (2013).
[7] Y. Takamura, T. Sakurai, R. Nakane, Y. Shuto, and S. Sugahara, J. Appl. Phys. **109**, 07B768 (2011).
[8] F. Y. Yang, C. H. Shang, C. L. Chien, T. Ambrose, J. J. Krebs, G. A. Prinz, V. I. Nikitenko, V. S. Gornakov, A. J. Shapiro, and R. D. Shull, Phys. Rev. B **65**, 174410 (2002).
[9] W. H. Wang, M. Przybylski, W. Kuch, L. I. Chelaru, J. Wang, Y. F. Lu, J. Barthel, H. L. Meyerheim, and J. Kirschner, Phys. Rev. B **71**, 144416 (2005).
[10] S. Kawagishi, T. Uemura, Y. Imai, K.-I. Matsuda, and M. Yamamoto, J. Appl. Phys. **103**, 07A703 (2008).
[11] M. S. Gabor, T. Petrisor, C. Tiusan, M. Hehn, and T. Petrisor, Phys. Rev. B **84**, 134413 (2011).
[12] S. Trudel, O. Gaier, Y. Hamrle, and B. Hillebrands, J. Phys. D: Appl. Phys. **43**, 193001 (2010).
[13] W. Wang, H. Sukegawa, R. Shan, T. Furubayashi, and K. Inomata, Appl. Phys. Lett. **92**, 221912 (2008).
[14] S. Trudel, G. Wolf, J. Hamrle, B. Hillebrands, P. Klaer, M. Kallmayer, H.-J. Elmers, H. Sukegawa, W. Wang, and K. Inomata, Phys. Rev. B **83**, 104412 (2011).
[15] S. Trudel, J. Hamrle, B. Hillebrands, T. Taira, and M. Yamamoto, J. Appl. Phys. **107**, 043912 (2010).